JACS
JOURNAL OF THE AMERICAN CHEMICAL SOCIETY
Article
pubs.acs.org/JACS

Quantitative Measurements of HO_2 and Other Products of *n*-Butane Oxidation (H_2O_2, H_2O, CH_2O, and C_2H_4) at Elevated Temperatures by Direct Coupling of a Jet-Stirred Reactor with Sampling Nozzle and Cavity Ring-Down Spectroscopy (cw-CRDS)

Mokhtar Djehiche,[†] Ngoc Linh Le Tan,[†] Chaithanya D. Jain,[†] Guillaume Dayma,[†] Philippe Dagaut,*[,†] Christian Chauveau,[†] Laure Pillier,[†] and Alexandre Tomas[‡]

[†]ICARE, INSIS, CNRS, 1c Avenue de la recherche scientifique, 45071 Orléans cedex 2, France

[‡]Ecole Nationale Supérieure des Mines de Douai, 941 Rue Charles Bourseul, 59508 Douai cedex, France

ABSTRACT: For the first time quantitative measurements of the hydroperoxyl radical (HO_2) in a jet-stirred reactor were performed thanks to a new experimental setup involving fast sampling and near-infrared cavity ring-down spectroscopy at low pressure. The experiments were performed at atmospheric pressure and over a range of temperatures (550−900 K) with *n*-butane, the simplest hydrocarbon fuel exhibiting cool flame oxidation chemistry which represents a key process for the auto-ignition in internal combustion engines. The same technique was also used to measure H_2O_2, H_2O, CH_2O, and C_2H_4 under the same conditions. This new setup brings new scientific horizons for characterizing complex reactive systems at elevated temperatures. Measuring HO_2 formation from hydrocarbon oxidation is extremely important in determining the propensity of a fuel to follow chain-termination pathways from R + O_2 compared to chain branching (leading to OH), helping to constrain and better validate detailed chemical kinetics models.

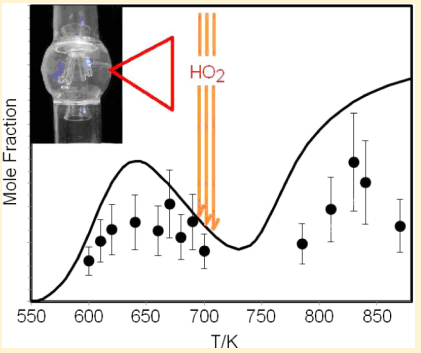

1. INTRODUCTION

Hydroperoxyl radicals (HO_2) play an important role in both atmospheric and combustion chemistry.[1,2] These radicals contribute to the formation of H_2O_2 (2 $HO_2 \rightarrow H_2O_2 + O_2$) that is considered to play a key role for the ignition in homogeneous charge compression ignition (HCCI) engines. There, the chain-terminating reaction H + O_2 + M → HO_2 + M consumes most of the H atoms, and the main chain-branching reaction (H + O_2 → O + OH) is relatively unimportant. The ignition would be caused by H_2O_2 decomposition (H_2O_2 → OH + OH). Also, when exhaust gas recirculation is used in internal combustion engines to reduce NO_x emissions, HO_2 plays a complex role via its reaction with NO: NO + HO_2 → NO_2 + OH.[3] To better assess the importance of these processes during the combustion of fuels, quantitative measurements of HO_2 are highly desirable. Whereas such measurements[4−6] have been performed in chemical systems operating around room temperature, difficulties appear at elevated temperature where HO_2 seems to be too reactive to be quantitatively measured after sampling. Previous efforts involved the use of the indirect fluorescence assay by gas expansion (FAGE) technique where HO_2 reacts with NO to yield OH that is measured by laser-induced fluorescence[7] and dual-modulation Faraday spectroscopy.[8,9] In this work, we built a new experimental setup based on a room temperature demonstrator described earlier[10] to measure HO_2 radicals by cavity ring-down spectroscopy with continuous wave light (cw-CRDS).[11] Beside the measurements of HO_2 concentrations during the oxidation of *n*-butane, more stable species were quantified under the same conditions using a simple and affordable technique. These measurements of stable species are similar to what was reported earlier for H_2O_2,[12,13] H_2O,[12] CH_2O,[12] and C_2H_4.[12]

2. EXPERIMENTAL SECTION

The experimental setup involves two parts: (i) a jet stirred reactor (JSR)-sampling nozzle assembly and (ii) a low-pressure cw-cavity ring-down spectrometer.

2.1. The JSR-Sampling Nozzle Assembly. A fused silica spherical JSR with a volume of 37 cm^3 (Figure 1) was used. The stirring is achieved by four jets exiting 0.5 mm i.d. injectors nozzles. Details of the development and operation of such rector can be found in an earlier publication by Dagaut et al.[14] The reactor design is based on the construction rules proposed by David et al.[15] and Matras et al.[16] The residence time for the gas mixture inside the reactor can be varied from a few milliseconds to seconds by changing the total inlet gas flow. Total length of the reactor including the side arms is 75 cm. The reactor is heated by a 30 cm regulated electrical oven that can reach 1200 K. The oven is surrounded by ceramic wool. The temperature along the main axis of the reactor is measured by a movable thermocouple (type K). The reactants were high-purity oxygen (99.995% pure form Air Liquide) and high-purity *n*-butane (>99.5% pure from Air Liquide). The reactants were diluted with nitrogen (<100 ppm of H_2O, <50 ppm of O_2, <1000 ppm Ar, <5 ppm of H_2 from Air Liquide) and mixed just before entering the injectors. The fuel−nitrogen mixture flowed through a capillary, whereas the O_2/N_2

Received: October 18, 2014
Published: November 7, 2014

   dx.doi.org/10.1021/ja510719k | J. Am. Chem. Soc. 2014, 136, 16689−16694

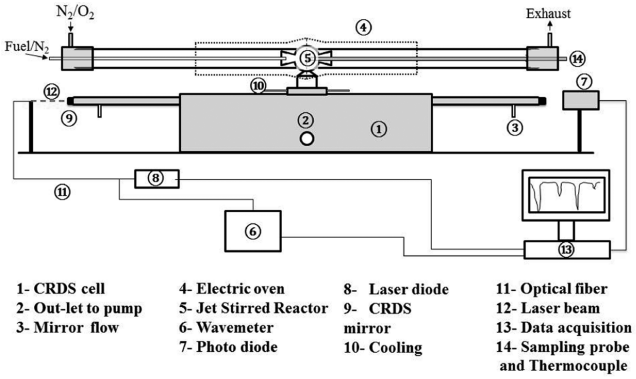

Figure 1. Simplified scheme of the experimental setup.

mixture flowed in the reactor extension tube (Figure 1). Mass flow controllers (Brooks 5850TR) were used to deliver the gases that were preheated before injection to minimize temperature gradients inside the reactor. To determine the concentrations of different species formed during the combustion process, the gas mixture is sampled with the CRDS cell through a fused silica nozzle (100 μm tip orifice, 53° angle; the tip is located ca. 5 mm inside the reactor) fixed between the JSR and the CRDS cell.

The CRDS cell is kept at low pressure (0.3 to 10 ± 10% mbar), whereas the reactor operates at atmospheric pressure. A rotary vane pump was used to withdraw samples from the reactor. The flow through the sampling cone was ca. 70 cm^3/min, whereas the total flow rate entering the reactor ranged from ca. 1400 to 4500 cm^3/min. A high-precision gauge was used to measure the cell pressure (THYRACONT vd85, 1200 to 5×10^{-4} (±0.3−10%) mbar). The expansion of the gas sample into the CRDS cell causes a pressure drop and cooling which both slow chemical reactions. This helps detecting highly reactive species such as free radicals. The volume (approximately 3 L) of the detection cell was kept relatively high for such instruments in order to limit wall reactions. The connection of the nozzle to the CRDS cell is cooled by circulating a water−ethanol mixture (80:20) at 0−5 °C. This limits heat transfer from the reactor to the CRDS cell and prevents O-ring degradation (Figure 1).

2.2. The cw-Cavity Ring-Down Spectrometer. CRDS has been well adopted by the scientific community in the past decades to carry out a variety of measurements.[17,18] Only a brief description of the technique is given here. Two ultrareflective mirrors (AT Films, 1 m radius of curvature, 99.999% reflectivity) are mounted on a rectangular cuboid separated by 74 cm to form an optical resonator (Figure 1). A continuous laser light source emitted by a DFB laser emitting at around 1510 nm (Fitel, 40 mW) was used as a light source. The laser diode is tunable over a 3 nm interval using a temperature and current controller (Newport, model 6100). A key point in cw-CRDS is the frequency matching between the laser emission and a cavity mode: this condition was achieved by mounting one of the mirrors onto a ring-shaped piezoelectric transducer fed with a triangular voltage and modulating the length of the cavity over a free spectral range.[7] The light escaping from the cavity through the rear mirror is detected by an avalanche photodiode, and once the light exceeds a user-determined threshold, the laser beam is switched off using a fibered acousto-optic modulator (Optoelectronic). The light intensity is recorded by a data acquisition card (National Instruments PCI-6111E) with 200 ns time resolution, and the ring down time is determined through an exponential fitting using the Labview 2010 software (National Instruments Corp.). Ring-down times are then converted to absorbing species concentrations [A] using the following equation:

$$[A]_t = \frac{L}{d \times c \times \sigma}\left(\frac{1}{\tau_t} - \frac{1}{\tau_0}\right) \quad (1)$$

where σ is the absorption cross section at the absorbing wavelength, L the distance between the two cavity mirrors, d the length, over which the absorbing species is present, c is the speed of light, and τ_t and τ_0 are the ring-down times in the presence and absence of absorber, respectively. The absorption length (d) was determined by injecting known quantities of methane and acetylene and measuring the absorbance at the center of the absorption lines at 6623.18 cm^{-1} (Figure 2) and 6625.15 cm^{-1}, respectively.[19] We used absorption cross

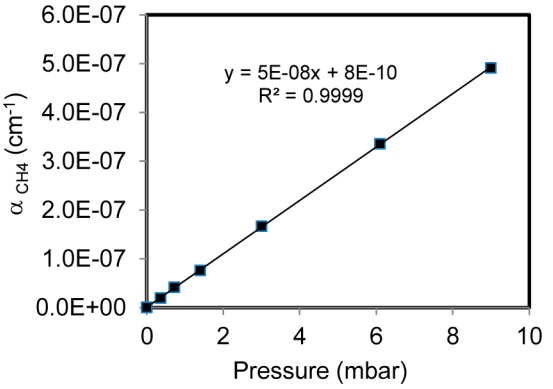

Figure 2. Measured absorption coefficient (α) of methane as a function of CRDS cell pressure at 9 cm of absorption path length.

sections of 1.54×10^{-23} and 7.8×10^{-22} cm^2 for CH_4 and C_2H_2, respectively, at 0.3−10 mbar (we took into account the variation of cross section with pressure) in the presence of a mirror protection nitrogen flow of 67 cm^3/min. An effective absorption length d = 9 ± 1.5 cm was determined.

The absorption cross section of HO_2 has been determined previously in air and helium (Table 1). Using an average HO_2 air-

Table 1. Line Strength, Cross Sections, and Pressure Broadening Coefficient of HO_2 at 6625.79 cm^{-1}

P_{ref}, mbar	80 (air)[20]	65 (He)[21]	40 (air)[20]
γ in cm^{-1} atm^{-1}	0.1	0.057	0.106
$S \times 10^{21}$ cm^{-1}	3.5	4.2	4.8
$\sigma \times 10^{19}$ cm^2 at P_{ref}	1.04	1.68	1.97

broadening coefficient of 0.106 cm^{-1}/atm,[20] it is possible to calculate the HO_2 absorption cross section at 6625.79 cm^{-1} and 0.3 mbar based on literature data. Using the most recent determination of Tang et al.[20] (30 Torr air), we calculated a value of 3.16×10^{-19} cm^2 for a line strength of 4.8×10^{-21}. Using the data from Johnson[22] (60 Torr air, see footnote c in Table 2 of Tang et al.)[20] and Thiébaud[21] (50 Torr He) enables to determine Doppler-limited cross sections of 2.45×10^{-19} and 2.58×10^{-19} cm^2, respectively. On the other hand, using the upper limit value of γ_{air} = 0.14 cm^{-1}/atm obtained by Ibrahim et al.,[23] yields a cross section of 3.56×10^{-19} cm^2 based on the determination of Tang et al.[20] Thus, we decided to use an average HO_2 absorption cross section of 3×10^{-19} cm^2 at 0.3 mbar air associated with an uncertainty of 0.6×10^{-19} cm^2 (i.e., 20%). A global uncertainty of about 40% may be expected taking into account the uncertainties on the literature data (about 20%).

At low fuel conversion and at 0.3 mbar in the CRDS cell, some stable species are not detectable. For that reason, we measured them at 10 mbar.

The absorption cross section of CH_2O at 6624.78 cm^{-1} has been calculated using $S = (9.1 \pm 1.8) \times 10^{-24}$ cm^{-1} [24] and γ = 0.1 cm^{-1}/atm.[25] We obtained a value of $\sigma = (5.1 \pm 0.5) \times 10^{-22}$ cm^2 at 10 mbar.

The cross section of water at 6621.5 cm^{-1} was calculated using a line strength of 6.69×10^{-24} cm^{-1} [19] and a broadening coefficient of 0.1 cm^{-1}/atm.[12] At 10 mbar this yields a water vapor cross section of $(2.9 \pm 0.1) \times 10^{-22}$ cm^2.

The cross sections of H_2O_2 and C_2H_4 have been determined previously by Bahrini et al.[12] For H_2O_2 at 1 mbar we considered that the cross section is the same in air and in He (γ_{He} = 0.068 cm^{-1}/

dx.doi.org/10.1021/ja510719k | J. Am. Chem. Soc. 2014, 136, 16689−16694

atm),[26] which allowed calculating the concentrations at 1 mbar. By changing the pressure to 10 mbar in air, the calculated absorption cross sections of H_2O_2 at 6624.1 cm^{-1} is $\sigma = (6.8 \pm 1.3) \times 10^{-23}$. Due to the absence of data for C_2H_4 (γ_{air} and S), we used the cross section obtained at 13 mbar published by Bahrini et al.[12] ($\sigma_{6623.37} = 3.6 \times 10^{-23}$ cm^2).

3. RESULTS AND DISCUSSION

Recently, Bahrini et al.[12] have studied the combustion of *n*-butane in similar conditions with a JSR connected to a CRDS cell via a microprobe and have reported the detection of stable species H_2O_2, CH_2O, C_2H_4, and H_2O. However, they failed to detect HO_2 due to probable losses in the sampling probe, which extended inside to the centerline of the reactor. This motivated us to take up this study again and try to measure HO_2 concentrations.

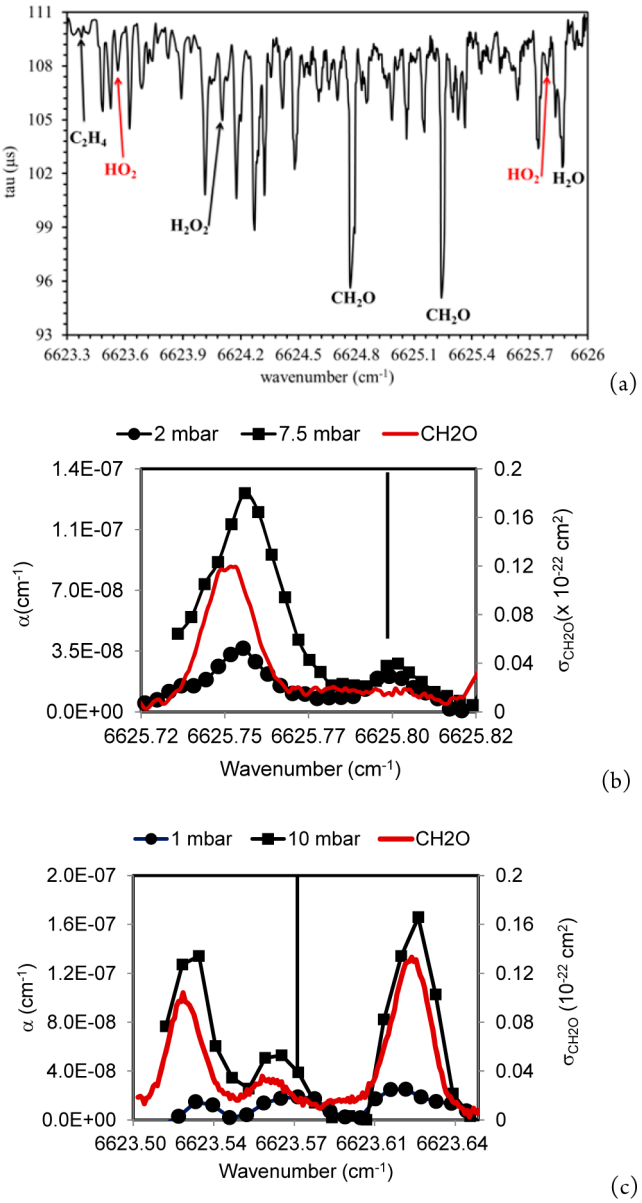

Figure 3. cw-CRDS spectra obtained during the oxidation of *n*-butane at 650 K. (a) Spectrum from 6623 to 6626 cm^{-1} (average of 50 ring-down events recorded at 3 mbar in the CRDS cell). (b) Effect of pressure in the CRDS cell on the absorption peaks of CH_2O and HO_2 at 6625.75 and 6625.79 cm^{-1}, respectively. (c) Effect of pressure on the absorption peaks of CH_2O (6623.52 and 6623.62 cm^{-1}) and of HO_2 at 6623.57 cm^{-1} at 1−10 mbar. Red line: formaldehyde absorption;[28] black symbol: absorption of combustion products (circles: at low pressure, squares: at higher pressure). The vertical lines indicate HO_2 absorption lines.

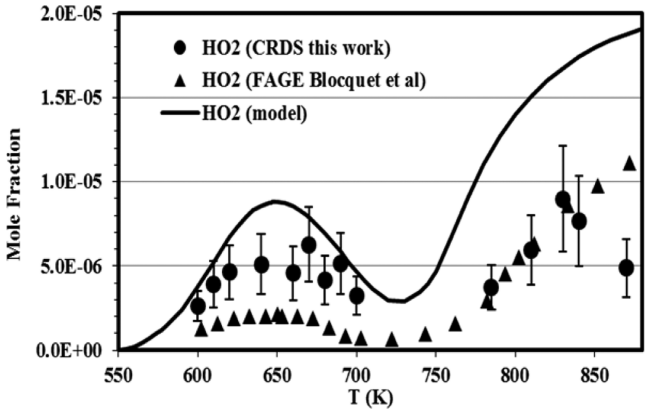

Figure 4. Concentrations profiles of HO_2 measured as a function of temperature during the oxidation of *n*-butane. Results from Blocquet et al.[7] obtained in similar conditions are shown for comparison. The results of a kinetic modeling using the PSR code[30] and our updated kinetic scheme[31] are also presented (lines).

To confirm our detection of HO_2 we carried out two series of experiments: (1) The oxidation of *n*-butane at 3% was performed at 650 K, in a jet-stirred reactor at 1 atm (φ = 0.5 and at mean residence time τ_R = 3s). Figure 3 shows a spectrum in the near IR region recorded by cw-CRDS (3%, φ = 0.5, 3s and 650 K). The absorption lines of HO_2, CH_2O, C_2H_4, H_2O_2, and H_2O in the range 6623 to 6626 cm^{-1} are identified (Figure 3a). This allows the detection of all these species using CRDS in the same conditions just by tuning the appropriate absorption wavelength. The hydroperoxyl radical is a very reactive species that is difficult to detect.[27] Generally when the total pressure is increased the signal corresponding to stable species increases, but that of radicals decreases because of their loss through increasingly fast chemical reactions.

Figure 3b,c shows the absorption peaks of CH_2O (6623.52, 6623.62 and 6625.74) and HO_2 at (6623.57 and 6625.79 cm^{-1}). We increased the pressure from 1 to 10 mbar to see the effect on absorption. It was observed that the formaldehyde absorption strongly increases with increasing pressure, while that was not the case for the signal attributed to the HO_2 radical. Since increasing the pressure in the CRDS cell has an adverse effect on radical detection, these results confirm that HO_2 radical is the species detected at 6623.57 and 6625.795 cm^{-1}. It was observed (Figure 3c) that stable species absorb at 6623.57 cm^{-1}, whereas that is not the case at 6625.795 cm^{-1} (Figure 3b). Therefore, we selected the absorption line at 6625.795 cm^{-1} for our measurements.

Reducing the pressure in the CRDS cell favors the measurement of HO_2 concentrations whereas a compromise with good sensitivity must be found. Therefore, the quantification of HO_2 was performed at a CRDS cell pressure of 0.3 mbar.

(2) A second series of experiments was performed for *n*-butane oxidation where we operated at (a) variable temperature and fixed equivalence ratio and (b) variable equivalence ratio and constant temperature. (a) First, we carried out the oxidation of *n*-butane under the same conditions as in the work of Bahrini et al.,[12] except they worked in helium, whereas

dx.doi.org/10.1021/ja510719k | J. Am. Chem. Soc. 2014, 136, 16689−16694

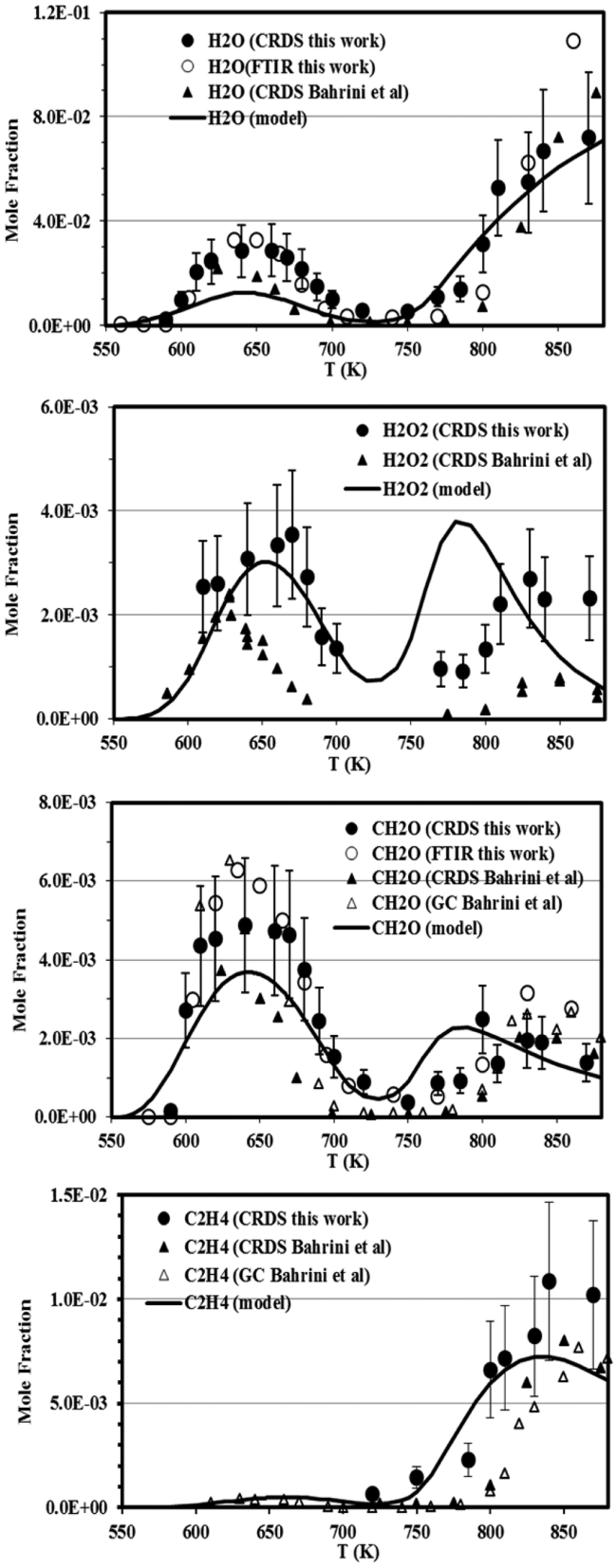

Figure 5. Concentrations profiles of stable intermediate species and products measured as a function of temperature during the oxidation of *n*-butane. Results from our FTIR measurements (see ref 29 for details) and those of Bahrini et al.[12] obtained in similar conditions are shown for comparison. The results of a kinetic modeling using the PSR code[30] and our updated kinetic scheme[31] are also presented (lines).

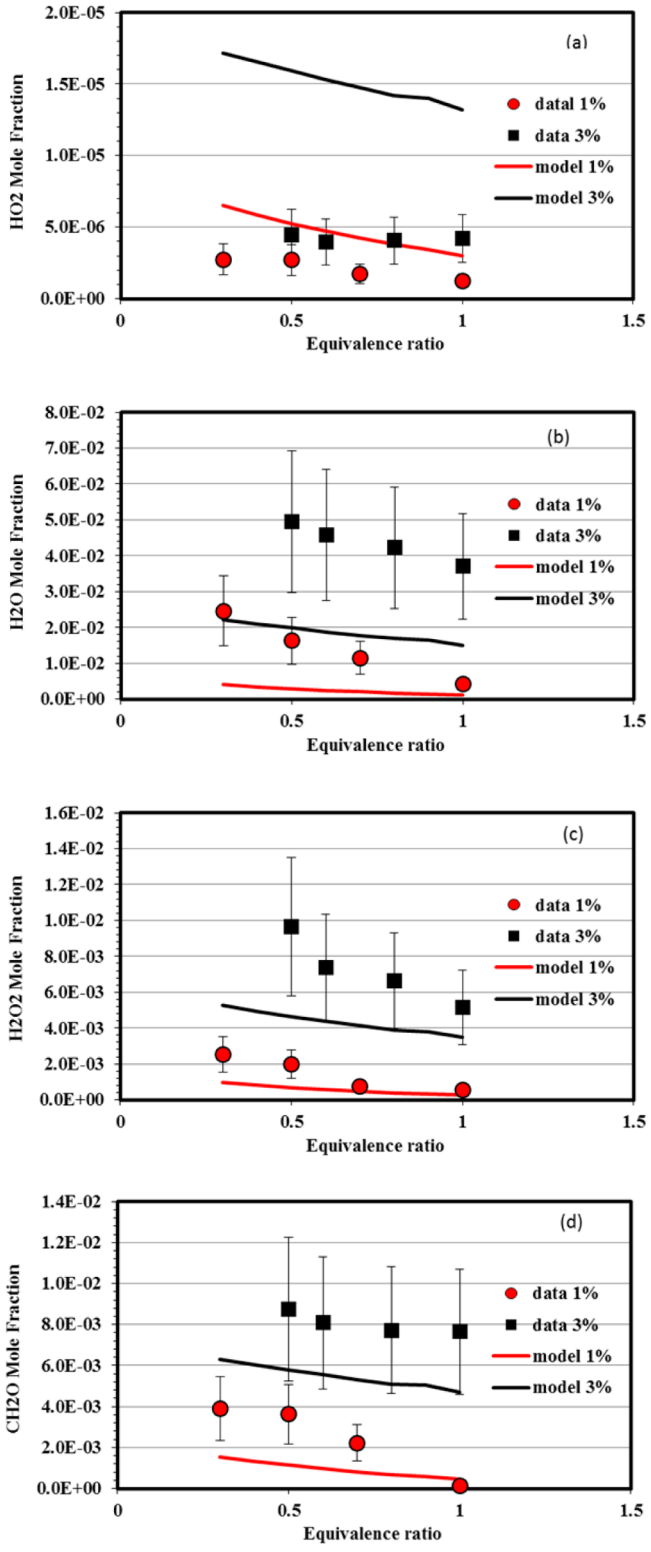

Figure 6. Comparison between experimental data (symbols) and computations[31] (lines) for (a) HO_2, (b)H_2O, (c) H_2O_2, and (d) CH_2O produced during the combustion of 3% *n*-butane (black squares and line) and 1% *n*-butane (red circles and line); φ = 0.3−1, τ_R = 3s, and T = 650 K.

the present experiments were performed in nitrogen. Quantification of oxidation products was performed as a function of temperature in the JSR. Figure 4 shows the measurements of different species sampled from the JSR

dx.doi.org/10.1021/ja510719k | J. Am. Chem. Soc. 2014, 136, 16689−16694

operating at 1 atm, over the temperature range 600−900 K, and at a mean residence time of 6 s. The reacting mixture molar composition was 2.3% *n*-butane, 14.95% oxygen, and 82.75% nitrogen. To confirm the reliability of the measurements by our CRDS technique the present results were compared with our FTIR measurements and the CRDS and gas chromatography (GC) results reported by Bahrini et al.[12] and the FAGE data of Blocquet et al.[7] Our measurements by CRDS were limited to 900 K for practical reasons. In the present experimental setup there are two potential sources of errors. The first one is the uncertainty in the reported absorption cross section for the given species (generally 10−20%),[12] and the second one is the uncertainty in the estimated effective absorption path length about 15% due to the fluctuation of total gas flow. Therefore, a maximum total uncertainty of 35% was assigned to all the measurements except HO_2, for which an uncertainty of 50% was estimated. In addition signal-to-noise ratio of the instrument also becomes important because of the low product yields during the combustion. To overcome this problem up to 150 ring-down events were averaged for each wavelength during the absorption line measurements. The noise in the baseline signal was around 0.2 μs, indicating a minimum measurable absorption coefficient $<7 \times 10^{-9}$ cm^{-1}.

For the first time HO_2 concentrations were measured during the oxidation of *n*-butane by cw-CRDS. Recently Bloquet et al.[7] have reported an indirect quantification of HO_2 during low temperature oxidation of *n*-butane using the FAGE technique which involves the conversion of HO_2 into OH by reaction with NO and detection of OH by laser-induced fluorescence. The comparison of these two sets of data (Figure 4) indicates that our measured HO_2 concentrations are ca. 50% higher than previously reported.[7] This difference might be due to losses of HO_2 during their probe sampling which differs from ours. Finally, one should also note that the present data are in reasonably good agreement with our model predictions. The kinetic model indicated that in helium the computed HO_2 mole fraction profiles are the same as in nitrogen up to 700 K. Above that temperature a shift of +10 K of the computed HO_2 profiles was observed, due to a reduction of H_2O_2 decomposition caused by the lower chaperon efficiency of helium versus nitrogen.

The measured concentrations of stable species formed during the same experiment are presented in Figure 5.

Water measurements performed at a CRDS cell pressure of 10 mbar are in good agreement with our FTIR data and previous CRDS measurements.[12] The model predictions are in good agreement with the measurements. The presently measured hydrogen peroxide concentrations (CRDS cell pressure = 10 mbar) were higher (ca. 30%) than those previously reported.[12] This difference might be due to losses of hydrogen peroxide during their microprobe sampling. Formaldehyde measurements performed at a CRDS cell pressure of 10 mbar are in good agreement with FTIR and GC measurements.

The model predictions are in good agreement with the present measurements in the cool flame region, whereas it slightly overestimates the formation of formaldehyde between 750 and 870 K. This results from an overestimation of the overall reactivity in this temperature range.

Finally, the ethylene concentration (measured at a CRDS cell pressure of 10 mbar) in the lower temperature region (<750 K) was lower than our detection limit, and hence only results obtained at higher temperatures could be compared to other measurements. A good agreement with the model predictions and other measurements was observed.

(b) The oxidation of *n*-butane (1% and 3% mole) was performed at a fixed temperature of 650 K, corresponding to the maximum of *n*-butane cool flame in the jet-stirred reactor. We operated at 1 atm, at a mean residence time τ_R = 3s, and the equivalence ratio was varied (φ = 0.3−1). Figure 6 shows the experimentally measured concentrations of HO_2, H_2O, H_2O_2, and CH_2O during the oxidation of *n*-butane (1% and 3% mole) in the JSR. For the CRDS measurements, the pressure in the cell was 10 mbar for measuring the stable species and 0.3 mbar to measure HO_2.

We observed that the concentrations of the measured species decrease when equivalence ratio increases, which corresponds to a reduced fuel conversion due to a reduction of the initial oxygen concentration. Also, we observed higher concentrations (∼3 times) of products formed when the initial fuel concentration is increased from 1% to 3% in mole. These observations follow both expectations and predictions obtained through detailed chemical kinetic modeling, although the computations do not match closely the data.

4. CONCLUSIONS AND PERSPECTIVES

A new experimental setup was built for measuring unstable species at elevated temperatures. The quantitative measurement of HO_2 at 550−900 K, by coupling of cw-CRDS and a jet-stirred reactor-sampling nozzle assembly, was performed for the first time thanks to the use of small tip orifice/wide angle sampling nozzle and very low pressure in the CRDS cell (0.3 mbar). The concentrations of H_2O_2, H_2O, CH_2O, and C_2H_4 were also measured using the same system (CRDS cell at 10 mbar) and found in good agreement with previously published measurements.

This new experimental setup will allow the measurement of concentrations of labile and stable species over a wide range of conditions (temperature, initial fuel concentration, equivalence ratio) and for a variety of fuels. These data will be useful for assessing the validity of combustion chemical kinetic models. Such studies are underway and the results should be presented in the near future.

AUTHOR INFORMATION

Corresponding Author

dagaut@cnrs-orleans.fr

Notes

The authors declare no competing financial interest.

ACKNOWLEDGMENTS

The research leading to these results has received funding from the European Research Council under the European Community's Seventh Framework Programme (FP7/2007-2013)/ERC grant agreement no. 291049-2G-CSafe. The authors thank Dr. C. Fittschen for useful discussions and Mr. P. Demaux, Dr. M. Idir, Mr. S. Thion, and Dr. C. Togbé for technical help.

REFERENCES

(1) Hucknall, D. J. *Chemistry of Hydrocarbon Combustion*, 1st ed.; Chapman and Hall: London, UK, 1985.

(2) Seinfeld, J. H.; Pandis, S. N. *Atmospheric Chemistry and Physics: From Air Pollution to Climate Change*, 2nd ed.; Wiley-Interscience: Hoboken, NJ, 2006.

(3) Dubreuil, A.; Foucher, F.; Mounaïm-Rousselle, C.; Dayma, G.; Dagaut, P. *Proc. Combust. Inst.* **2007**, *31*, 2879−2886.
(4) Clemitshaw, K. C. *Critical Rev. Environ. Sci. Technol.* **2004**, *34*, 1−108.
(5) Joens, J. A. *J. Phys. Chem.* **1994**, *98*, 1394−1397.
(6) Wallington, T. J.; Dagaut, P.; Kurylo, M. J. *Chem. Rev.* **1992**, *92*, 667−710.
(7) Blocquet, M.; Schoemaecker, C.; Amedro, D.; Herbinet, O.; Battin-Leclerc, F.; Fittschen, C. *Proc. Natl. Acad. Sci. U. S. A.* **2013**, *110*, 20014−20017.
(8) Brumfield, B.; Sun, W. T.; Wang, Y.; Ju, Y.; Wysocki, G. *Opt. Lett.* **2014**, *39*, 1783−1786.
(9) Kurimoto, N.; Brumfield, B.; Yang, X.; Wada, T.; Diévart, P.; Wysocki, G.; Ju, Y. *Proc. Combust. Inst.* **2015**; http://dx.doi.org/10.1016/j.proci.2014.05.120.
(10) Djehiche, M.; Le Tan, N. L., Tomas, A.; Pillier, L.; Idir, M.; Fittschen, C.; Dayma, G.; Dagaut, P. Proceedings of the European Combustion Meeting, Lund, Sweden, June 25−28, 2013; Combustion Institute: Pittsburgh, PA, 2013; Vol *6*, Paper P4-1, p 6
(11) Romanini, D.; Kachanov, A. A.; Sadeghi, N.; Stoeckel, F. *Chem. Phys. Lett.* **1997**, *264*, 316−322.
(12) Bahrini, C.; Morajkar, P.; Schoemaecker, C.; Frottier, O.; Herbinet, O.; Glaude, P.; Battin-Leclerc, F.; Fittschen, C. *Phys. Chem. Chem. Phys.* **2013**, *15*, 19686.
(13) Bahrini, C.; Herbinet, O.; Glaude, P.-A.; Schoemaecker, C.; Fittschen, C.; Battin-Leclerc, F. *J. Am. Chem. Soc.* **2012**, *134*, 11944−11947.
(14) Dagaut, P.; Cathonnet, M.; Rouan, J.-P.; Foulatier, R.; Quilgars, A.; Boettner, J.-C.; Gaillard, F.; James, H. *J. Phys. E: Sci. Instrum.* **1986**, *19*, 207−209.
(15) David, R.; Matras, D. *Can. J. Chem. Eng.* **1975**, *53*, 297−300.
(16) Matras, D.; Villermaux, J. *Chem. Eng. Sci.* **1973**, *28*, 129.
(17) Berden, G.; Peeters, R.; Meijer, G. *Int. Rev. Phys. Chem.* **2000**, *19*, 565−607.
(18) Brown, S. S. *Chem. Rev.* **2003**, *103*, 5219−5238.
(19) Rothman, L. S.; Jacquemart, D.; Barbe, A.; Chris Benner, D.; Birk, M.; Brown, L. R.; Carleer, M. R.; Chackerian, C., Jr.; Chance, K.; Coudert, L. H.; Dana, V.; Devi, V. M.; Flaud, J.-M.; Gamache, R. R.; Goldman, A.; Hartmann, J.-M.; Jucks, K. W.; Maki, A. G.; Mandin, J.-Y.; Massie, S. T.; Orphal, J.; Perrin, A.; Rinsland, C. P.; Smith, M. A. H.; Tennyson, J.; Tolchenov, R. N.; Toth, R. A.; Van der Auwera, J.; Varanasi, P.; Wagner, G. *J. Quant. Spec. Rad. Transfer* **2005**, *96*, 139−204.
(20) Tang, Y.; Tyndall, S. G.; Orlando, J. J. *J. Phys. Chem. A* **2010**, *114*, 369−378.
(21) Thiébaud, J.; Crunaire, S.; Fittschen, C. *J. Phys. Chem. A* **2007**, *111*, 6959−6966.
(22) Johnson, T. J.; Wienhold, F. G.; Burrows, J. P.; Burkhard, H. H. *J. Phys. Chem.* **1991**, *95*, 6499−6502.
(23) Ibrahim, N.; Thiébaud, J.; Orphal, J.; Fittschen, C. *J. Mol. Spectrosc.* **2007**, *242*, 64−69.
(24) Morajkar, P.; Schoemaecker, C.; Fittschen, C. *J. Mol. Spectrosc.* **2012**, *281*, 18−23.
(25) Barry, H. R.; Corner, L.; Hancock, G.; Peverall, R.; Ranson, T. L.; Ritchie, G. A. D. *Chem. Chem. Phys.* **2003**, *5*, 3106−3112.
(26) Jain, C. D. Laser photolysis coupled to detection by LIFf and cw-CRDS: Application to spectroscopic and kinetic studies of OH, HO_2, and HONO, Ph.D. Thesis, University of Lille I, Lille, France, 2011; https://ori-nuxeo.univ-lille1.fr/nuxeo/site/esupversions/db1a78c5-fb7f-422c-8a29-54a858c2e9fd.
(27) Djehiche, M.; Tomas, A.; Fittschen, C.; Coddeville, P. *Z. Phys. Chem.* **2011**, *225*, 983−992.
(28) Staak, M.; Gash, E. W.; Venables, D. S.; Ruth, A. A. *J. Mol. Spectrosc.* **2005**, *229*, 115−121.
(29) Galmiche, B.; Togbé, C.; Dagaut, P.; Halter, F.; Foucher, F. *Energy Fuels* **2011**, *25*, 2013−2021.
(30) Glarborg, P.; Kee, R. J.; Grcar, J. F.; Miller, J. A. *PSR: A FORTRAN Program for Modelling Well-Stirred Reactors*; Sandia National Laboratories: Livermore, CA, 1986, SAND86−8209.
(31) Dayma, G. unpublished results.